Building and evaluation of a PBPK model for Moclobemide in adults

Version	**1.1-OSP11.0**
based on *Model Snapshot* and *Evaluation Plan*	https://github.com/Open-Systems-Pharmacology/Moclobemide-Model/releases/tag/v1.1
OSP Version	11.0
Qualification Framework Version	2.3

This evaluation report and the corresponding PK-Sim project file are filed at:

https://github.com/Open-Systems-Pharmacology/OSP-PBPK-Model-Library/

Table of Contents

1 Introduction

The presented PBPK model of moclobemide has been developed to be used in a PBPK Drug-Drug-Interactions (DDI) network with moclobemide as a substrate and a moderate inhibitor of CYP2C19.

Moclobemide is a reversible inhibitor of monoamine oxidase A (RIMA), a drug primarily used to treat depression and social anxiety (Mayersohn 1995). Moclobemide pharmacokinetics is characterized by non-linearity in dose and time. Cmax concentrations decrease with dose for doses above 100 mg. Furthermore, a saturation in clearance at higher doses (200 mg and up) could be seen, as indicated by a longer terminal phase. In addition, multiple doses administration resulted in higher moclobemide concentrations compared to single dose. This could be indicative of the previously reported auto-inhibitory effect (Nair 1993).

Absorption: Moclobemide is highly soluble, and consequently fast and completely absorbed. Absolute bioavailability has been reported to be dependent on the dose, likely due to saturable (first-pass) metabolism (Mayersohn 1995).

Distribution: Moclobemide is moderately bound to plasma proteins and due to its lipophilicity distributes widely in the body (Vss ~ 1.2 L/kg) (MHRA Label Moclobemide).

Metabolism: About 99% of a dose is metabolized mainly via CYP2C19 (C-oxidation, producing metabolite RO12-8095) and FMO3 (N-oxidation, producing metabolite RO12-5637) (Gram 1995, Hoskins 2001, Mayersohn 1995).

Excretion: Less than 1% of a dose is excreted unchanged via the kidneys.

2 Methods

2.1 Modeling Strategy

The general workflow for building an adult PBPK model has been described by Kuepfer et al. (Kuepfer 2016). Relevant information on the anthropometry (height, weight) was gathered from the respective clinical study, if reported. Information on physiological parameters (e.g. blood flows, organ volumes, hematocrit) in adults was gathered from the literature and has been incorporated in PK-Sim® as described previously (Willmann 2007). The applied activity and variability of plasma proteins and active processes that are integrated into PK-Sim® are described in the publicly available 'PK-Sim® Ontogeny Database Version 7.3' (PK-Sim Ontogeny Database Version 7.3).

In general, the following step-wise workflow was followed:

1. Fit total hepatic CL as a placeholder using single dose i.v. (50 mg (Raaflaub 1984) and 150 mg (Schoerlin 1987)) data with renal clearance fixed to 0.034 ml/min/kg as derived from Schoerlin 1987 to select the appropriate distribution (i.e. partition coefficient) model.
2. Estimate the contribution of non-CYP2C19 mediated metabolism using data (p.o.) from CYP2C19 poor metabolizers (PM) (Yu 2001, Gram 1995). This pathway is assumed to be mainly attributed to FMO (flavin-containing monooxygenase) – however, also other unspecific CL would be captured here. An Asian individual was used for simulations of data reported by Yu 2001.
3. Use single dose data (i.v. and p.o.) to estimate Vmax and Km of CYP2C19.
4. Predict concentrations after multiple oral dosing and compare to literature. Steady state levels were not predicted very well, and the model was refined by including time-dependent auto-inhibition to account for a change in CL over time.
5. Predict single and multiple doses profiles (both i.v. and p.o.) with the updated model and compare to published profiles. Qualify model by comparing predicted CL/F and Cmax to the corresponding parameters in a review across multiple studies. Population prediction to verify the variability components of the model.

A typical European male subject (age = 30 years, weight = 73 kg, height = 176 cm, BMI = 23.57 kg/m2) was created in PK-Sim using the predefined database “European (ICRP, 2002)”, by adding CYP2C19 (PK-Sim RT PCR database) and FMO (other) expression and used in simulations, until stated otherwise. For simulations of Asian subjects, a typical Asian individual (Age = 30 y, weight = 60.03 kg, height = 169.96 cm, BMI = 20.78 kg/m2) was created from the predefined database “Asian (Tanaka, 1996)” by adding CYP2C19 (PK-Sim RT PCR database) and FMO (other) expression.

For simulations of the Ignjatovic 2009 data set, a typical European female subject (Age = 30 years, weight = 64 kg, height = 163 cm, BMI = 24.09 kg/m2) was created from the predefined database “European (ICRP, 2002)” by adding CYP2C19 (PK-Sim RT PCR database) and FMO (other) expression.

Initially, attempts were made to also unravel the contribution of the FMO3-specific clearance pathway and the unspecific pathway using the in vitro FMO-CL of moclobemide in a microsomal assay reported by Hoskins 2001. However, this route was abandoned as predictions were not in line with observations, potentially requiring the need for an in vivo - in vitro scaling factor. For the purpose of DDI predictions, the details of the CYP2C19 pathway only were considered relevant.

Population simulations were carried out to evaluate if the variability incorporated in the model matches the literature reports. A population of 2000 Asian subjects with age and weight in the same range as reported by Yu 2001 (age: 20-36 years, weight: 40-120 kg, 13% female) was generated, and the concentration time profile following a single dose of 300 mg p.o. was simulated for each virtual subject and summarized as mean +/- SD. The simulation was also performed for CYP2C19 poor metabolizers.

Details about input data (physicochemical, *in vitro* and clinical) can be found in Section 2.2.

Details about the structural model and its parameters can be found in Section 2.3.

2.2 Data

2.2.1 In vitro and physico-chemical data

A literature search was performed to collect available information on physico-chemical properties of moclobemide, see Table 1.

Parameter	Unit	Value	Source	Description
MW^{+}	g/mol	268.74	DrugBank DB01171	Molecular weight
$pK_{a,base}{}^{+}$		6.2	IPCS ICHEM	Acidic dissociation constant
Solubility $(pH)^{+}$	mg/mL	3 (6.8)	Moclobemide, INCHEM	Aqueous Solubility
logD		1.79	Pons 1990	Distribution coefficient
fu^{+}	%	50	MHRA Label Moclobemide	Fraction unbound in plasma
Km_FMO (microsomes)	mmol/L	0.77	Hoskins 2001	
Vmax_FMO (microsomes)	nmol/min/mg prot.	1.39	Hoskins 2001	
Renal Elimination	ml/min/kg	0.03	Schoerlin 1987	Schoerlin reports 2.6 ml/min/76kg
Ki_CYP2C19 (free)	µmol/L	203.8	Kramer-Nielsen 1996	The total ki value reported by Kramer was 210 umol/L and corrected with an fu_mic of 0.97

Table 1: Physico-chemical and *in-vitro* metabolization properties of moclobemide extracted from literature. $^{+}$*: Value used in final model*

2.2.2 Clinical data

A literature search was performed to collect available clinical data on moclobemide in adults, see Table 2.

Source	Route	Dose [mg]/ Schedule *	Pop.	Age [yrs] (mean or range)	Weight [kg] (mean or range)	Sex	N	Form.	Comment
Gram 1995+	p.o.	300 s.d. / b.i.d.	HV	26	-	m/f	8	tablet	EM + PM
Yu 2001+	p.o.	300 s.d.	HV-Asian	-	60.3	m	8	tablet	EM, PM and EM+OMP40
Wiesel 1985+	p.o.	50, 100, 200 s.d.	HV or patient etc	26.3	75.8	m	6	tablet	
Ignjatovic 2009	p.o.	150 t.i.d.	Pat	-	-	m/f	6	tablet	
Dingemanse 1998	p.o.	300 s.d.	HV	-	-	f/m	12	tablet	
Schoerlin 1987+	p.o. & i.v. infusion	150 t.i.d. /s.d.	HV	27	76	m	12	tablet/ solution	
Guentert 1990+	p.o.	150 t.i.d.	HV	19-29	59-86	m/f	14	tablet	
Raaflaub 1984+	p.o. & i.v. infusion	50 s.d.	HV	42	4	m	6	tablet/ solution	

Table 2: Literature sources of clinical concentration data of moclobemide used for model development and validation. *-: respective information was not provided in the literature source; *:single dose unless otherwise specified; EM: extensive metabolizers; PM: poor metabolizers; +: Data used for final parameter identification*

2.3 Model Parameters and Assumptions

2.3.1 Absorption

Particle dissolution for the formulation has been selected.

2.3.2 Distribution

Physico-chemical parameters were set to the reported values (see Section 2.2.1). It was assumed that the major binding partner in plasma is albumin.

After testing the available organ-plasma partition coefficient and cell permeability calculation methods available in PK-Sim, observed clinical data were best described by choosing the partition coefficient calculation by `Rodgers and Rowland` and cellular permeability calculation by `PK-Sim Standard`.

2.3.3 Metabolism and Elimination

Two metabolic pathways were implement in the model:

- Saturable CYP2C19 mediated metabolization.
- Linear FMO mediated to account for lumped non-CYP metabolization.

Data after repeated dosing indicates some sort of time-dependent elimination. The addition of an inhibitory metabolite may be an explanation. However, it would be very challenging to incorporate the kinetics of such a metabolite in the existing model, taking into account that no data on IC50 or Ki are available for such a metabolite. Therefore, it was decided to account for the time-dependency by simply including a time-dependent autoinhibition on CYP2C19 enzyme system.

Given the available data, the parameters Kinact and Kinact_half defining the time-dependent autoinhibition could not be estimated together (not separately identifiable). Assuming Kinact is enzyme but not substance specific, it was decided to fix Kinact to the value reported by Wu 2014 for omeprazole and only estimate Kinact_half.

2.3.4 Automated Parameter Identification

Following parameter values were estimated for the base model:

- Km_2C19
- Vmax_2C19
- Intrinsic Clearance FMO (i.e. non CYP2C19 metabolism)
- $Kinact_{half}$ CYP2C19 for time-dependent autoinhibition

3 Results and Discussion

The next sections show:

1. Final model input parameters for the building blocks: Section 3.1.
2. Overall goodness of fit: Section 3.2.
3. Simulated vs. observed concentration-time profiles for the clinical studies used for model building and for model verification: Section 3.3.

3.1 Final input parameters

The parameter values of the final PBPK model are illustrated below.

Formulation: Moclobemide tablet

Type: Particle Dissolution

Parameters

Name	Value	Value Origin
Thickness (unstirred water layer)	20 µm	Publication-Willmann S, Thelen K, Becker C, et al. Mechanism-based prediction of particle size-dependent dissolution and absorption: cilostazol pharmacokinetics in dogs. Eur J Pharm Biopharm. 2010 Sep;76(1):83-94 https://doi.org/10.1016/j.ejpb.2010.06.003
Type of particle size distribution	Monodisperse	
Particle radius (mean)	10 µm	

Compound: Moclobemide

Parameters

Name	Value	Value Origin	Alternative	Default
Solubility at reference pH	3 mg/ml	Internet-Moclobemide, INCHEM	Measurement	True
Reference pH	6.8	Internet-Moclobemide, INCHEM	Measurement	True
Lipophilicity	1.79 Log Units	Publication-Pons 1990	logD	True
Fraction unbound (plasma, reference value)	0.5	Other-MHRA Label Moclobemide	Measurement	True
Cl	1	Database-DrugBank DB01171		
Is small molecule	Yes			
Molecular weight	268.74 g/mol	Database-DrugBank DB01171		
Plasma protein binding partner	Albumin			

Calculation methods

Name	Value
Partition coefficients	Rodgers and Rowland
Cellular permeabilities	PK-Sim Standard

Processes

Metabolizing Enzyme: CYP2C19-Intrinsic-CL_MM_fit

Species: Human
Molecule: CYP2C19

Parameters

Name	Value	Value Origin
Vmax (liver tissue)	2.03 µmol/min/kg tissue	Parameter Identification
Km	1.11 µmol/l	Parameter Identification

Metabolizing Enzyme: FMO_other-Intrinsic-CL-fit

Species: Human
Molecule: FMO_other

Parameters

Name	Value	Value Origin
Intrinsic clearance	0.24 l/min	Parameter Identification

Systemic Process: Renal Clearances-Schoerlin 1987

Species: Human

Parameters

Name	Value	Value Origin
Fraction unbound (experiment)	0.5	
Plasma clearance	0.034 ml/min/kg	Publication-Schoerlin 1987

Inhibition: CYP2C19-Kramer-unbound

Molecule: CYP2C19

Parameters

Name	Value	Value Origin
Ki	203.82 µmol/l	Publication-Kramer-Nielsen 1996

Inhibition: CYP2C19-TimeDep_AutoInh-fit

Molecule: CYP2C19

Parameters

Name	Value	Value Origin
kinact	5 1/h	Publication-Wu2014
K_kinact_half	94.85 µmol/l	Parameter Identification

3.2 Diagnostics Plots

The following section displays the goodness-of-fit visual diagnostic plots for the PBPK model performance of all data listed in Section 2.2.2.

The first plot shows observed versus simulated plasma concentration, the second weighted residuals versus time.

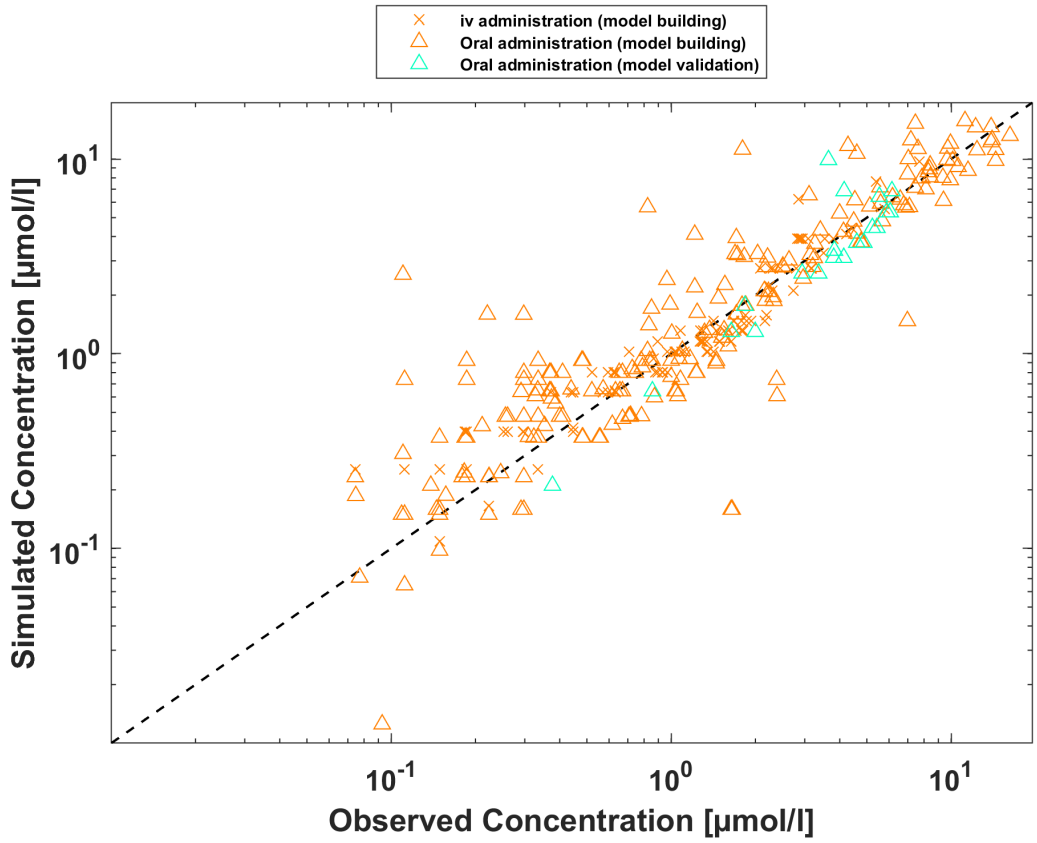

Moclobemide concentration in plasma

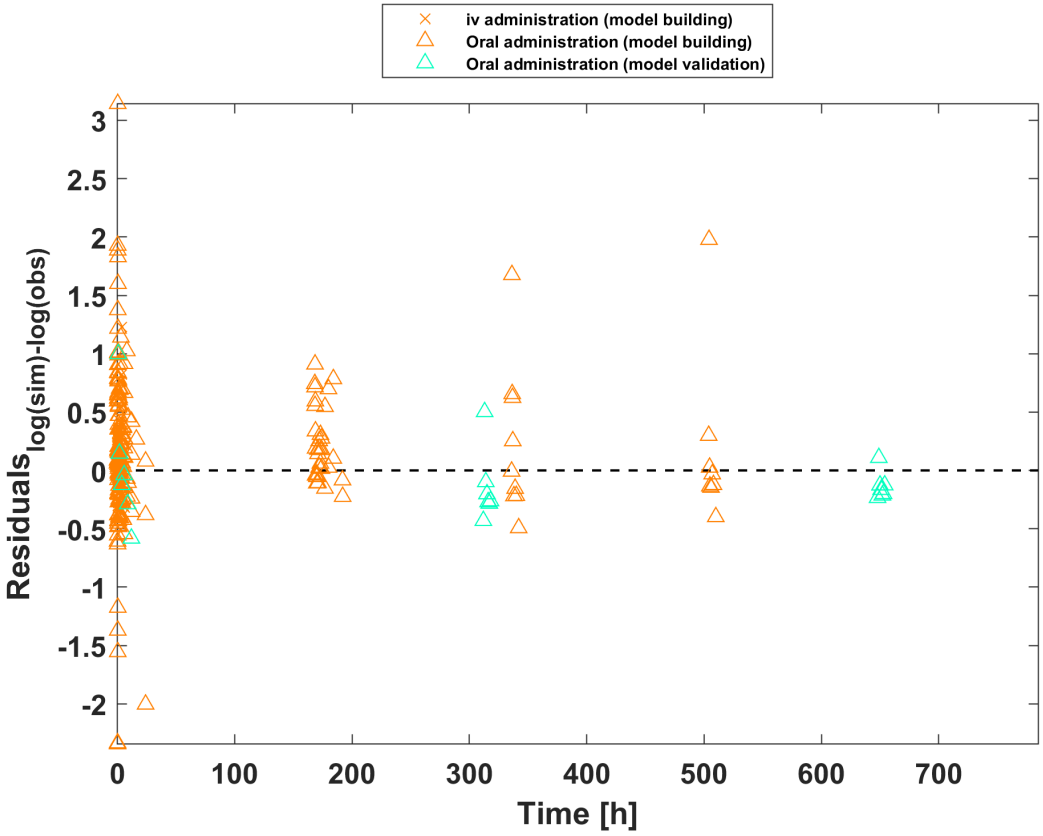

Moclobemide concentration in plasma

GMFE = 1.455257

3.3 Concentration-Time Profiles

Simulated versus observed concentration-time profiles of all data listed in Section 2.2.2 are presented below.

3.3.1 Model Building

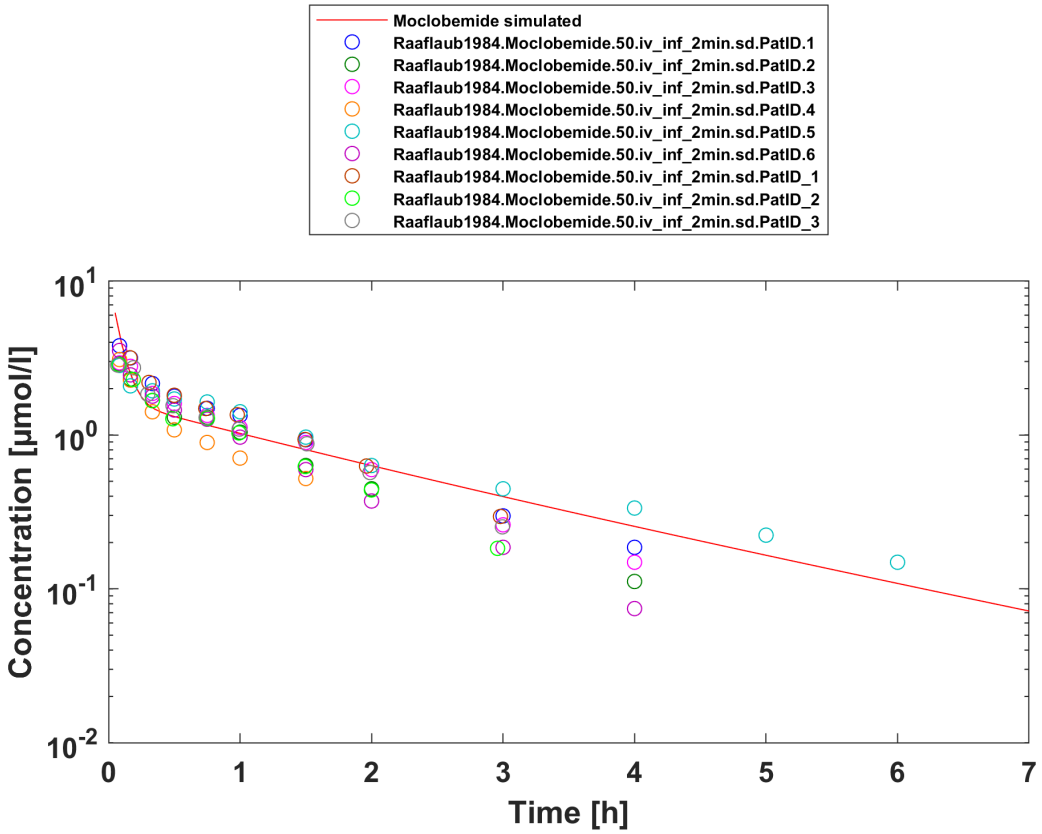

50 mg moclobemide iv

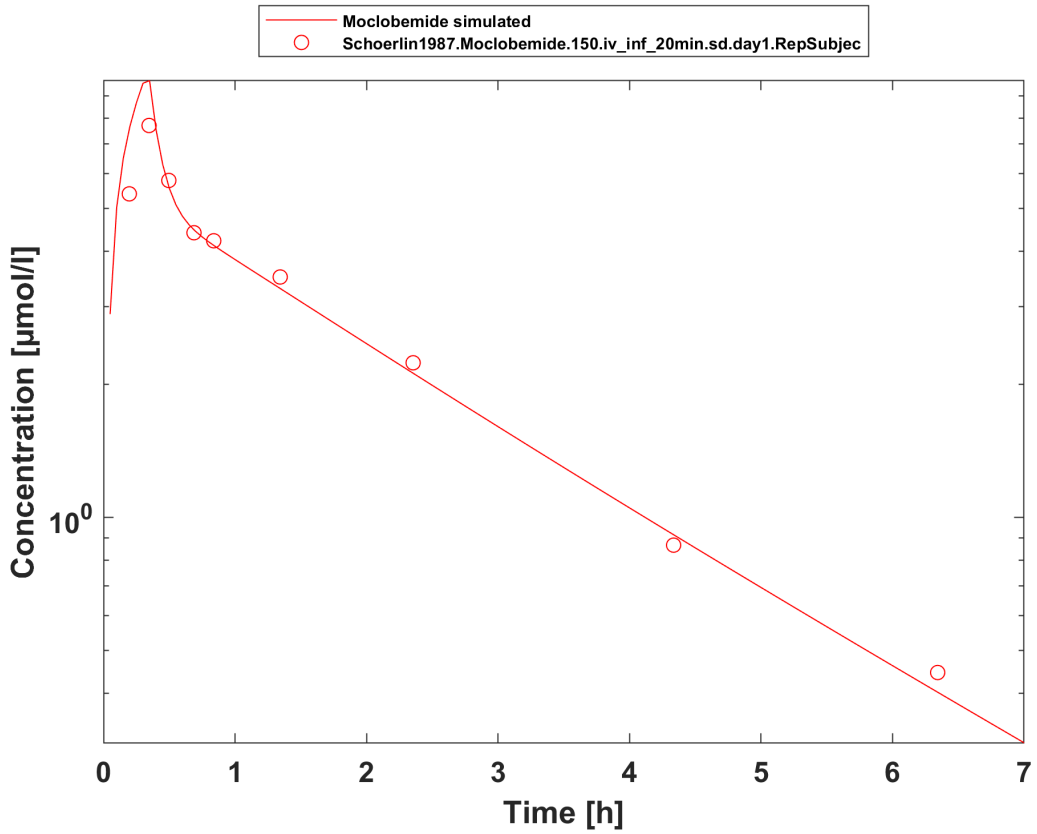

150 mg moclobemide iv 20min

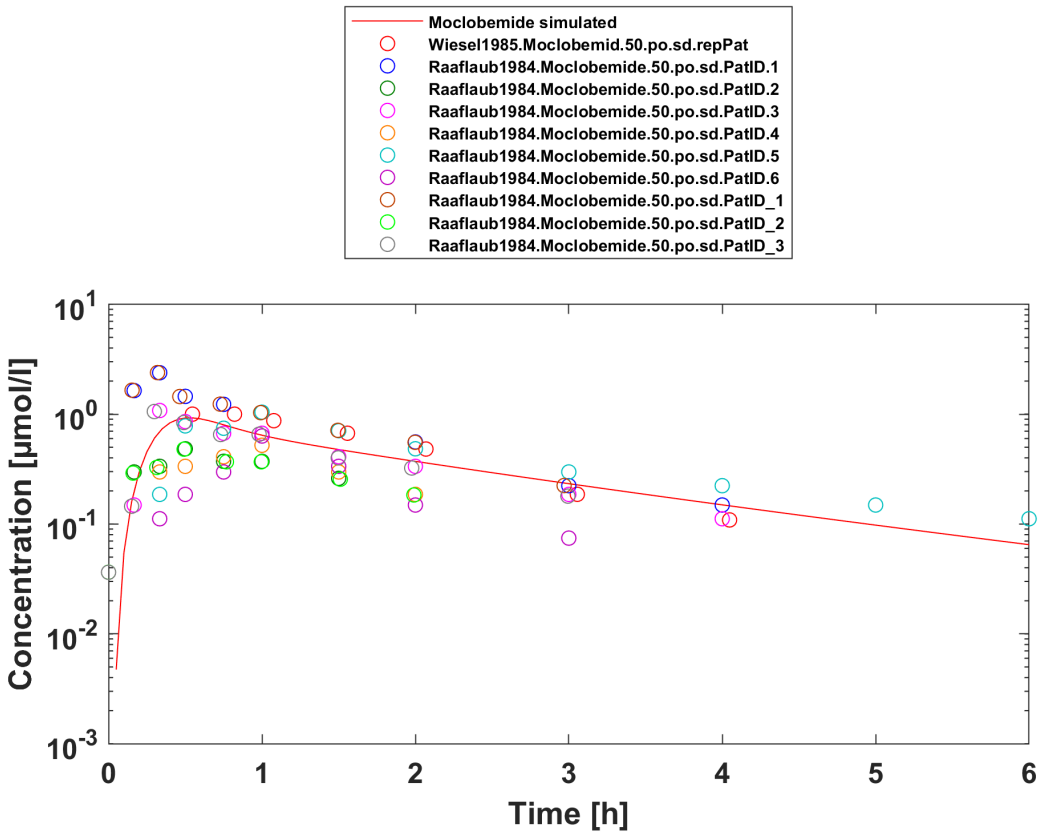

50 mg moclobemide po

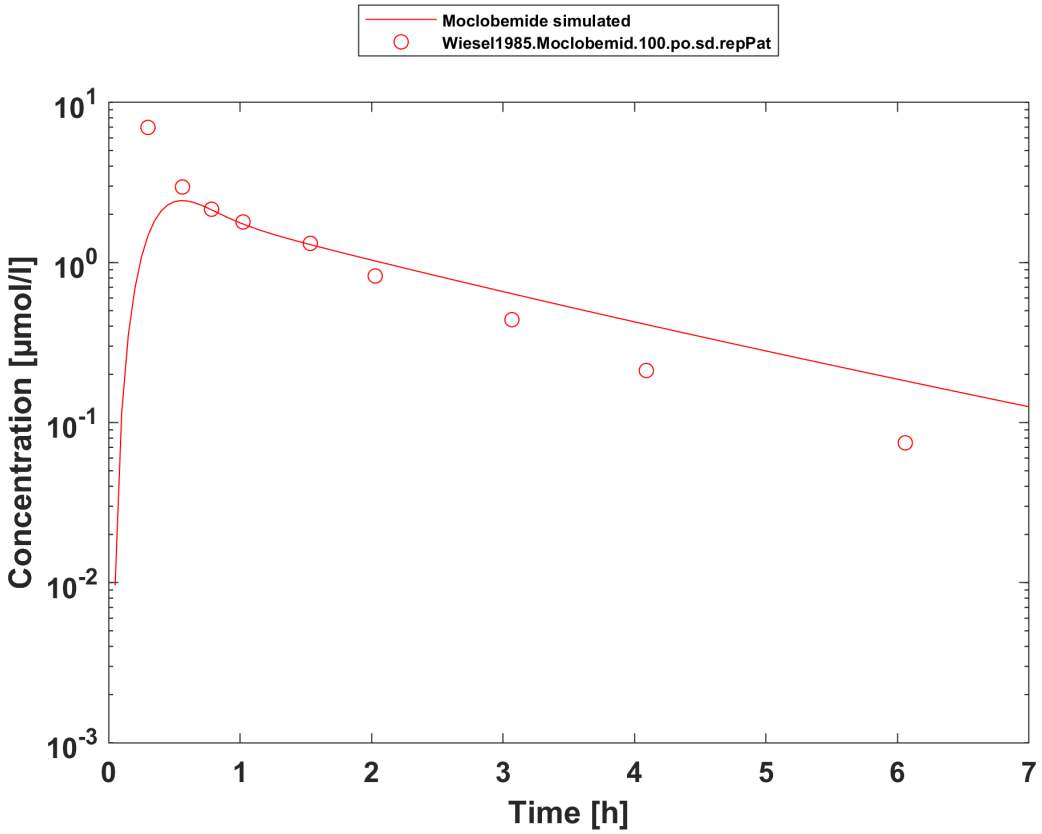

100 mg moclobemide po

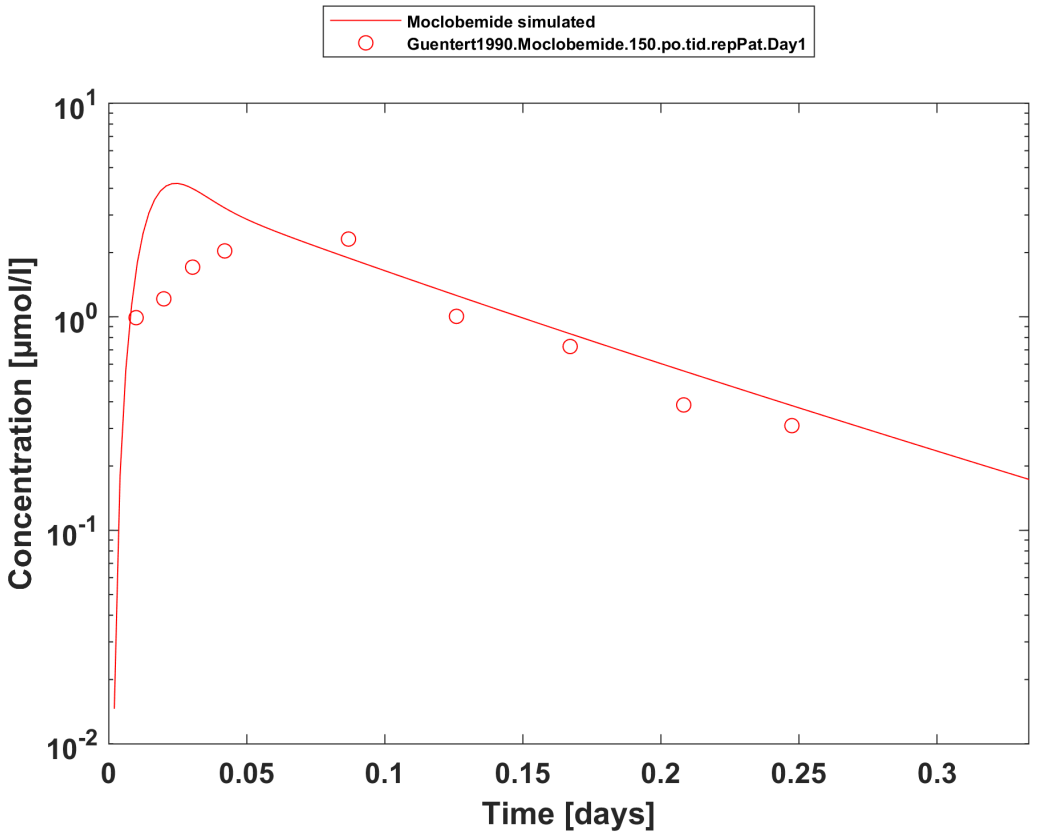

150 mg moclobemide po

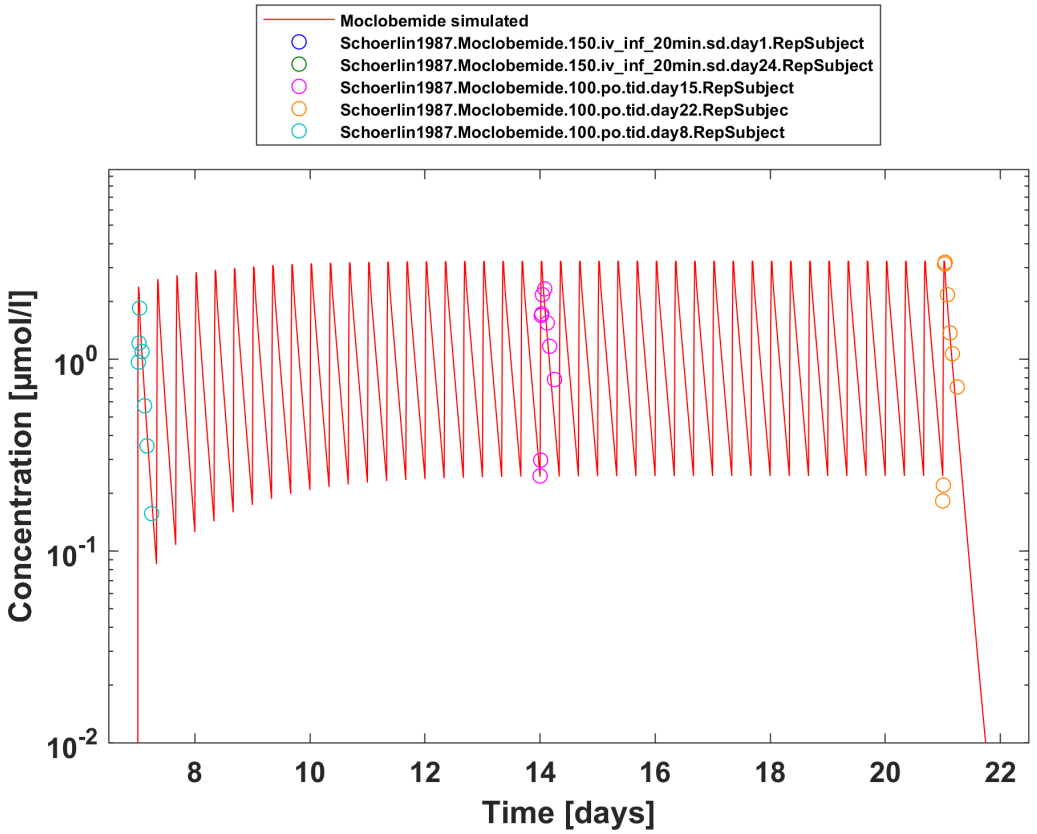

150 mg moclobemide po 14d

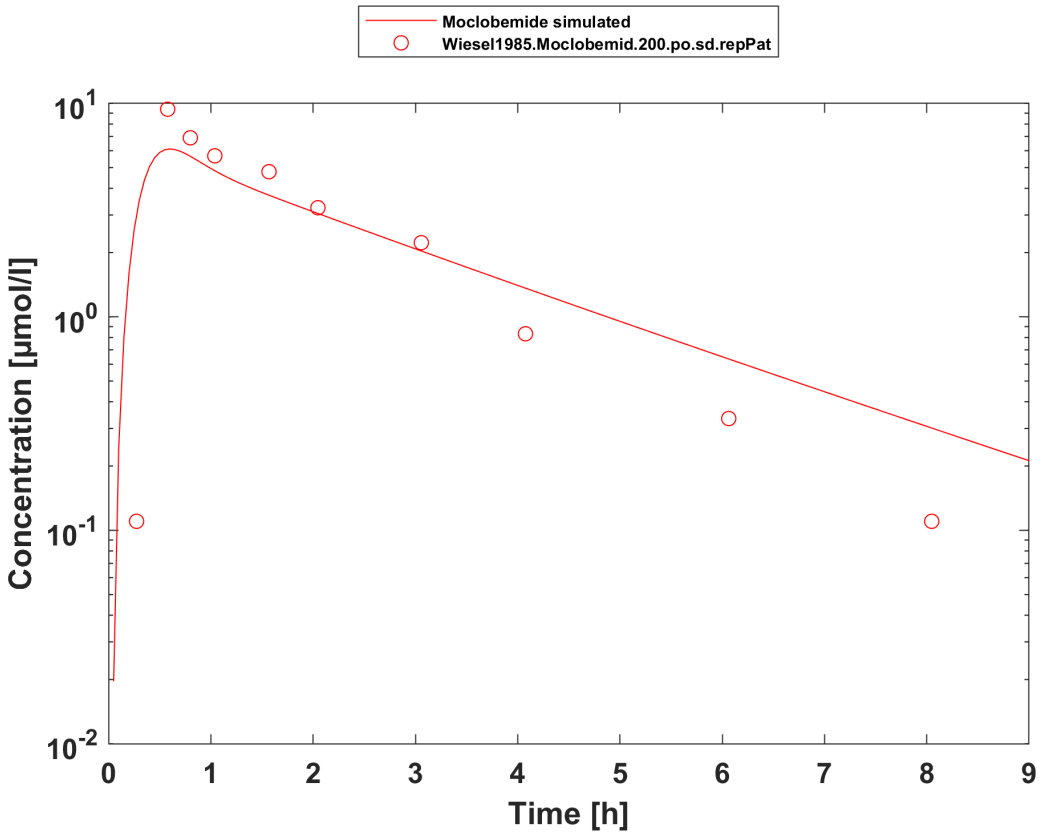

200 mg moclobemide po

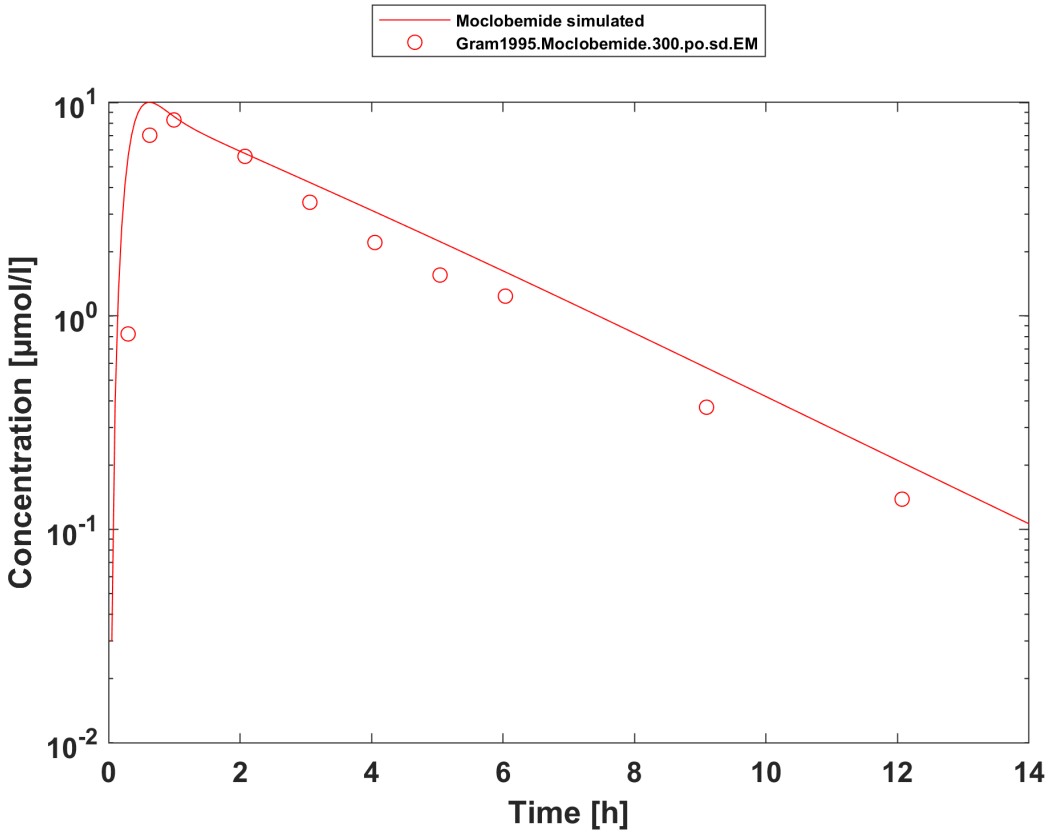

300 mg moclobemide po

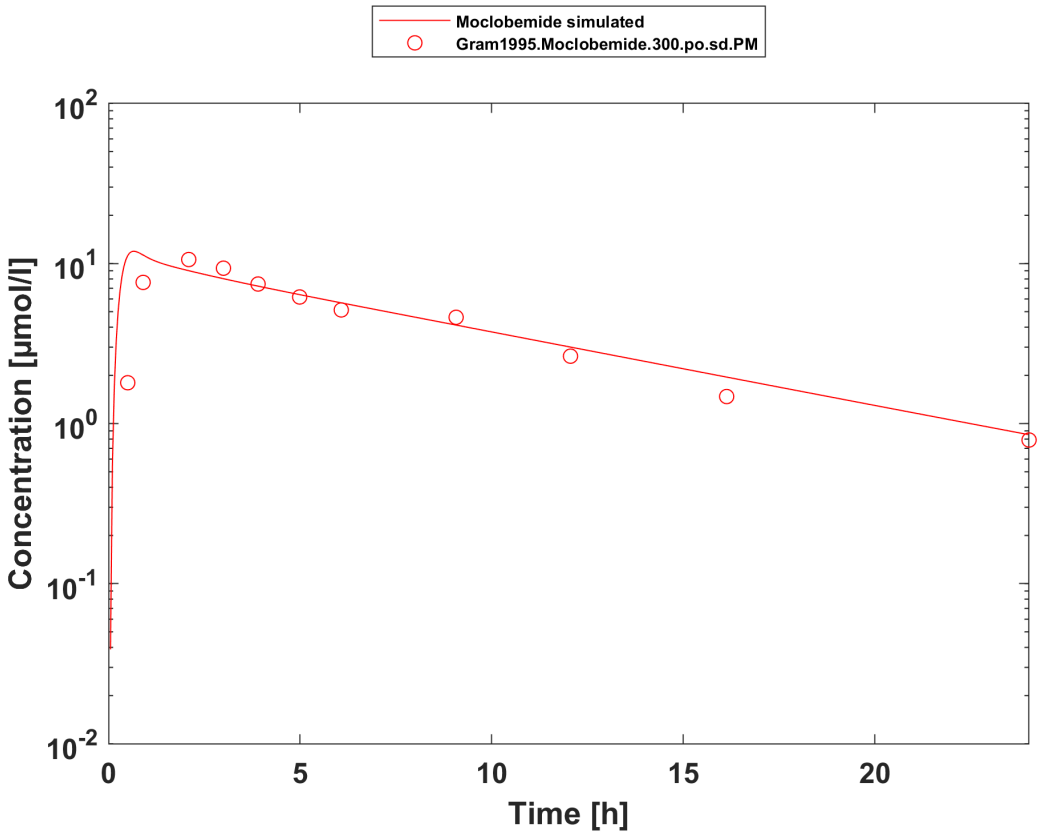

300 mg moclobemide po PM

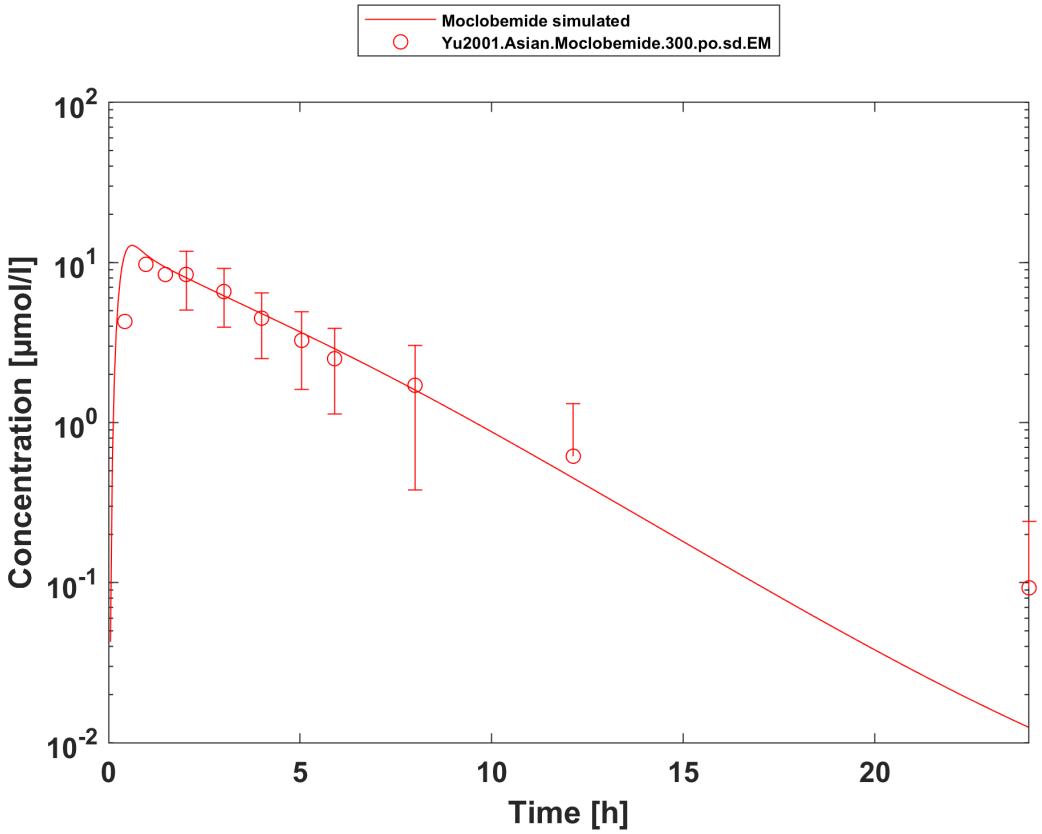

300 mg moclobemide po asian

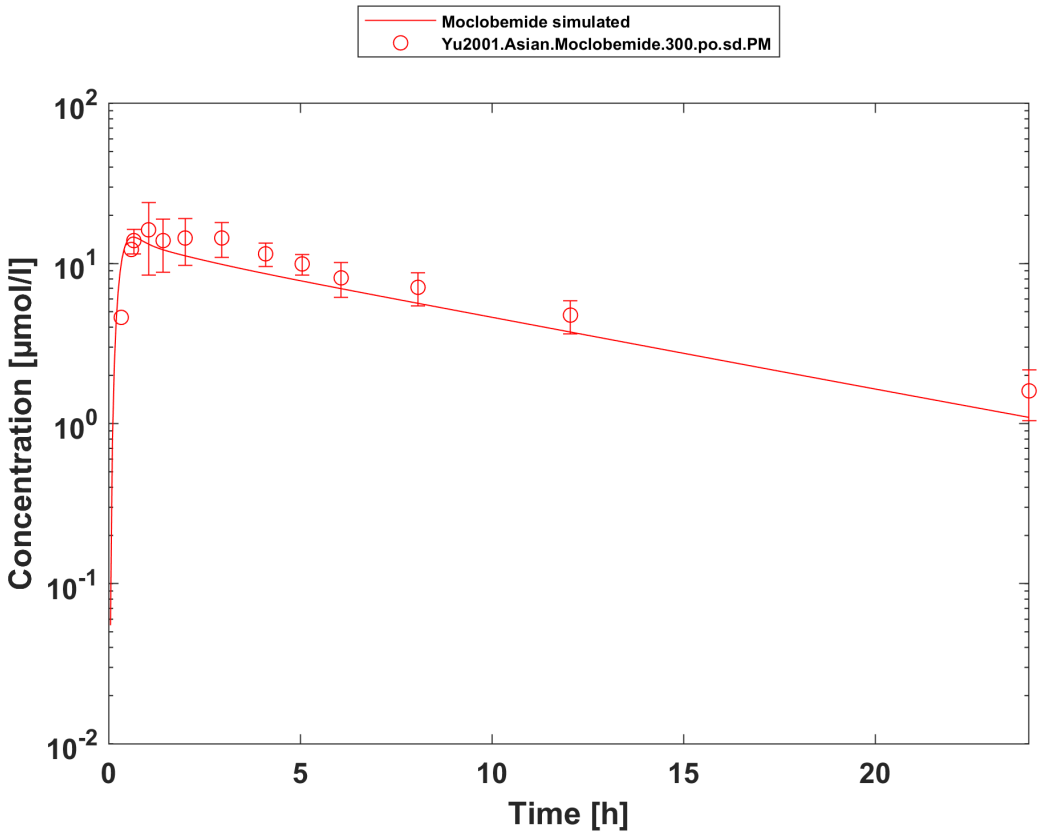

300 mg moclobemide po asian PM

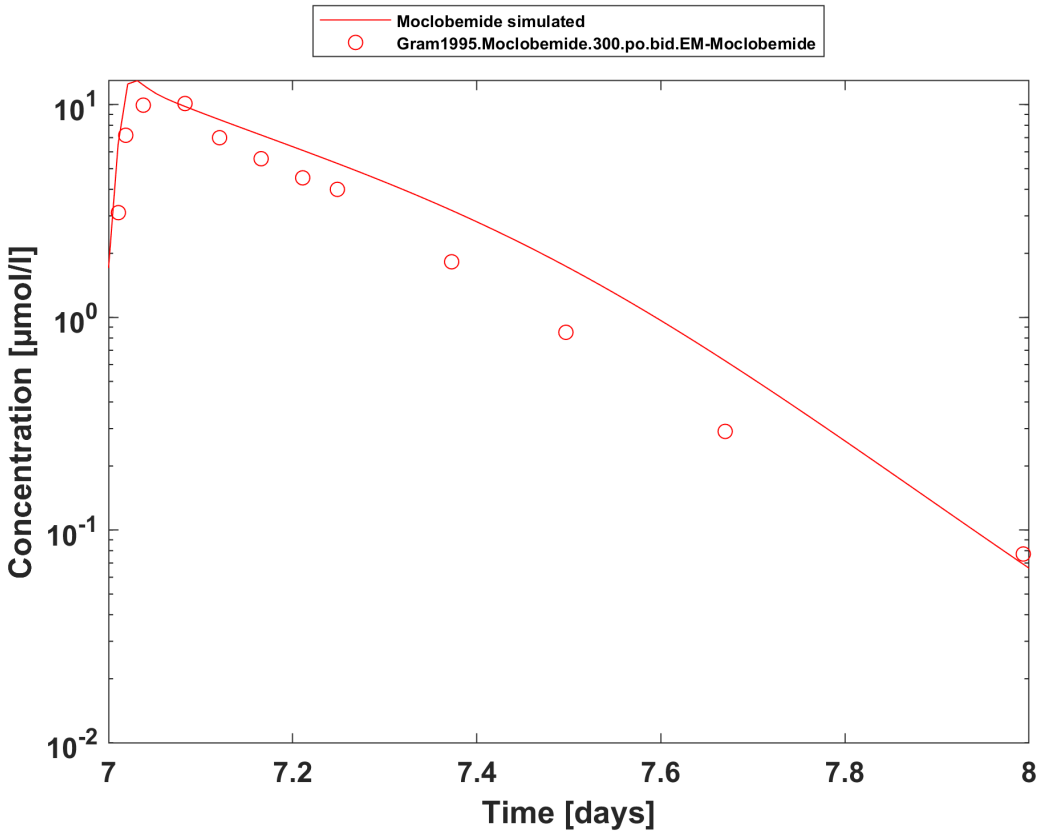

300 mg moclobemide po 7d

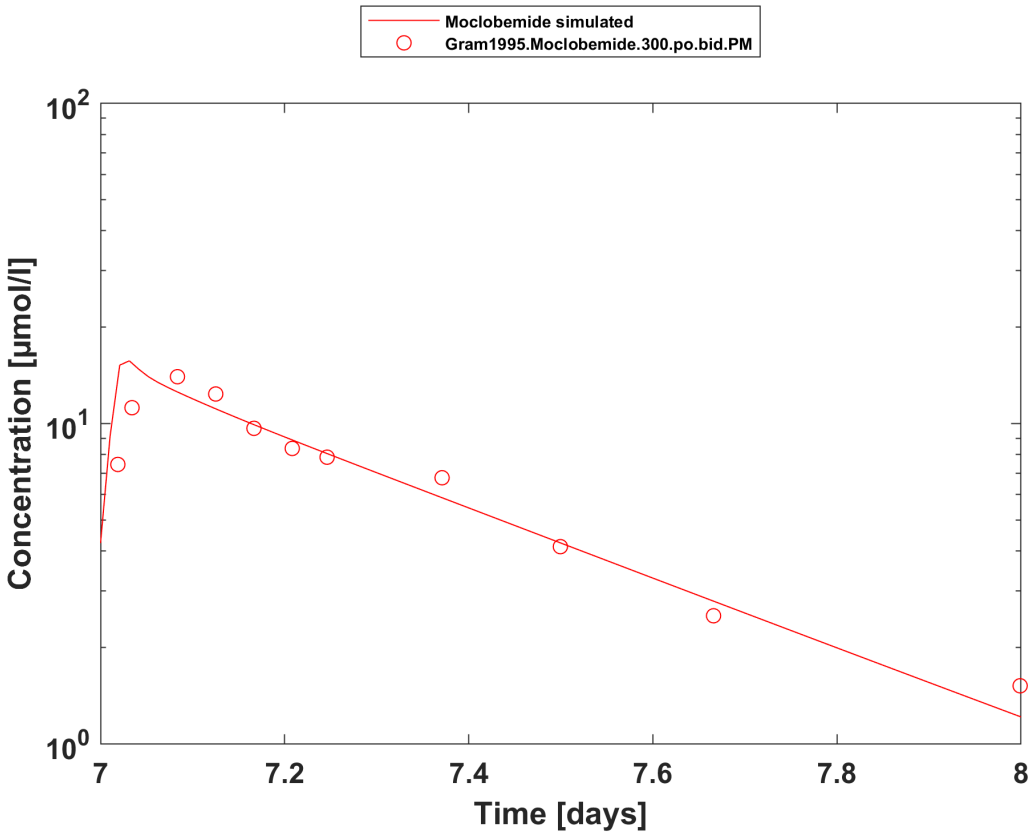

300 mg moclobemide po PM 7d

3.3.2 Model Verification

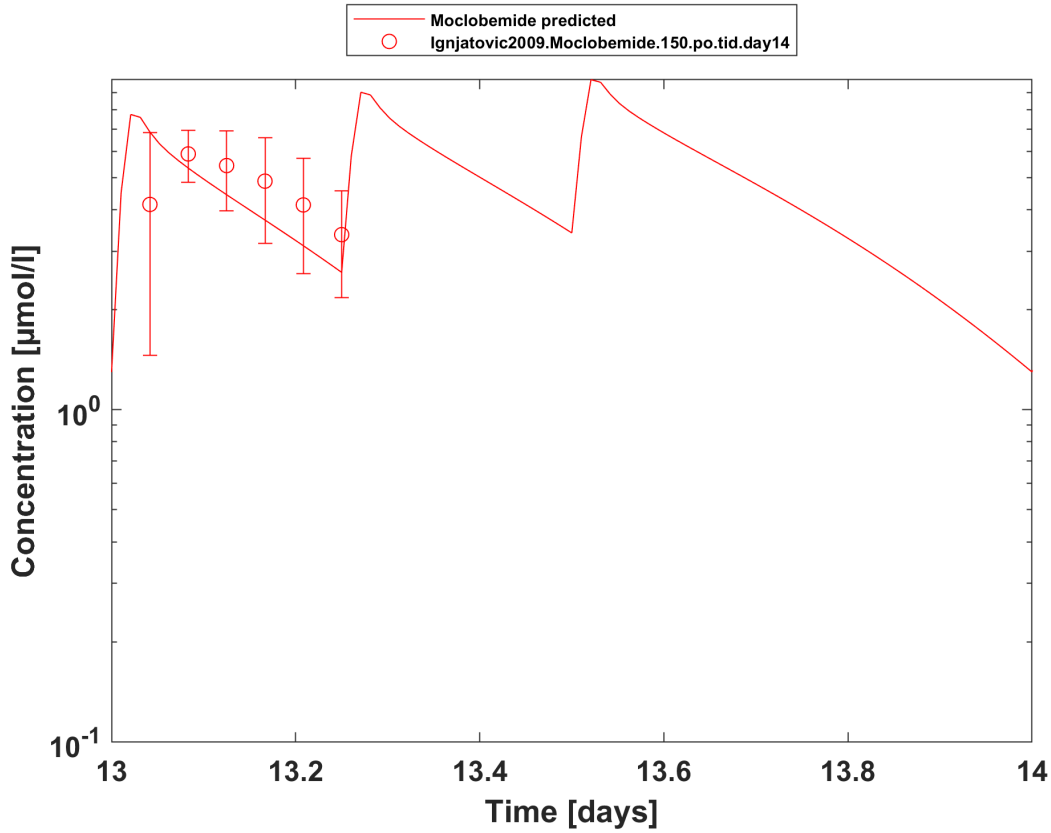

150 mg moclobemide po female day14

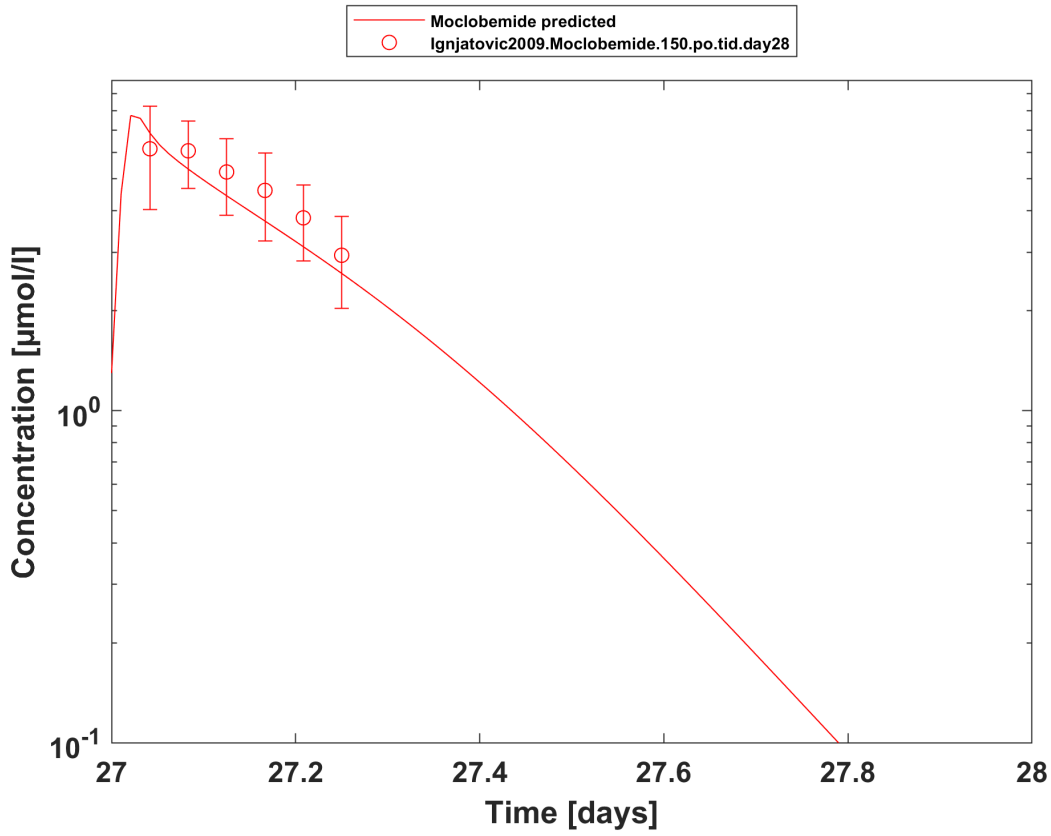

150 mg moclobemide po female day28

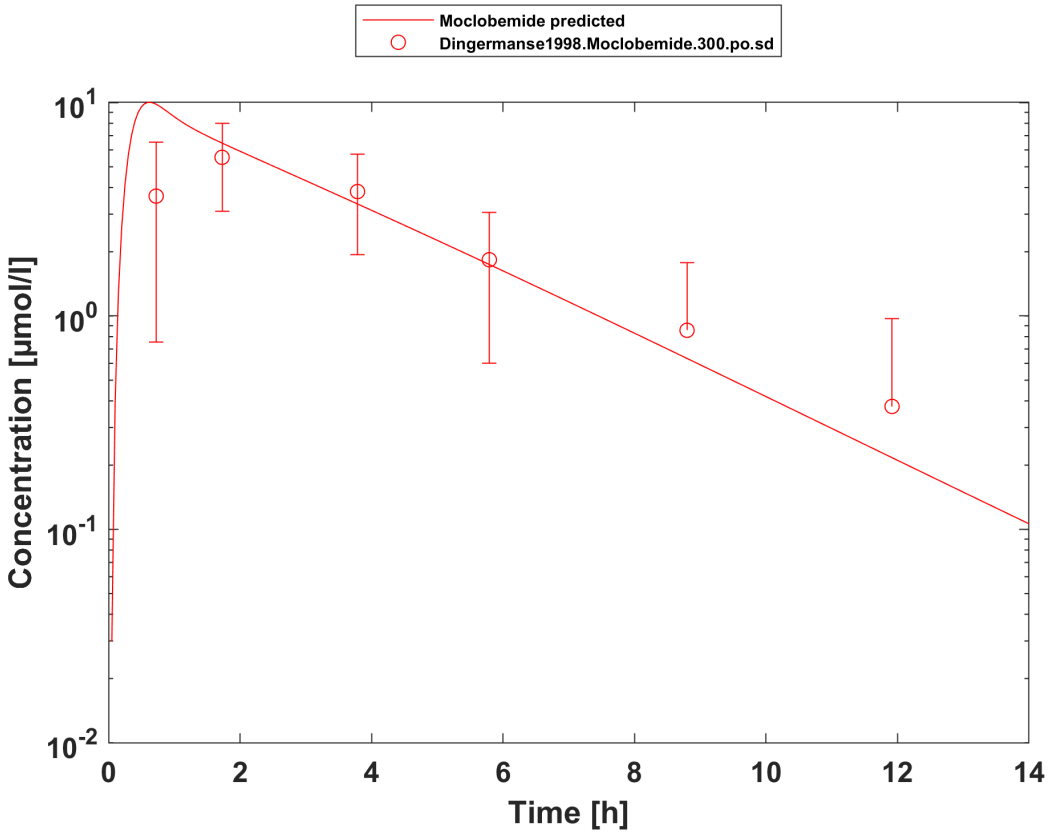

300 mg moclobemide po

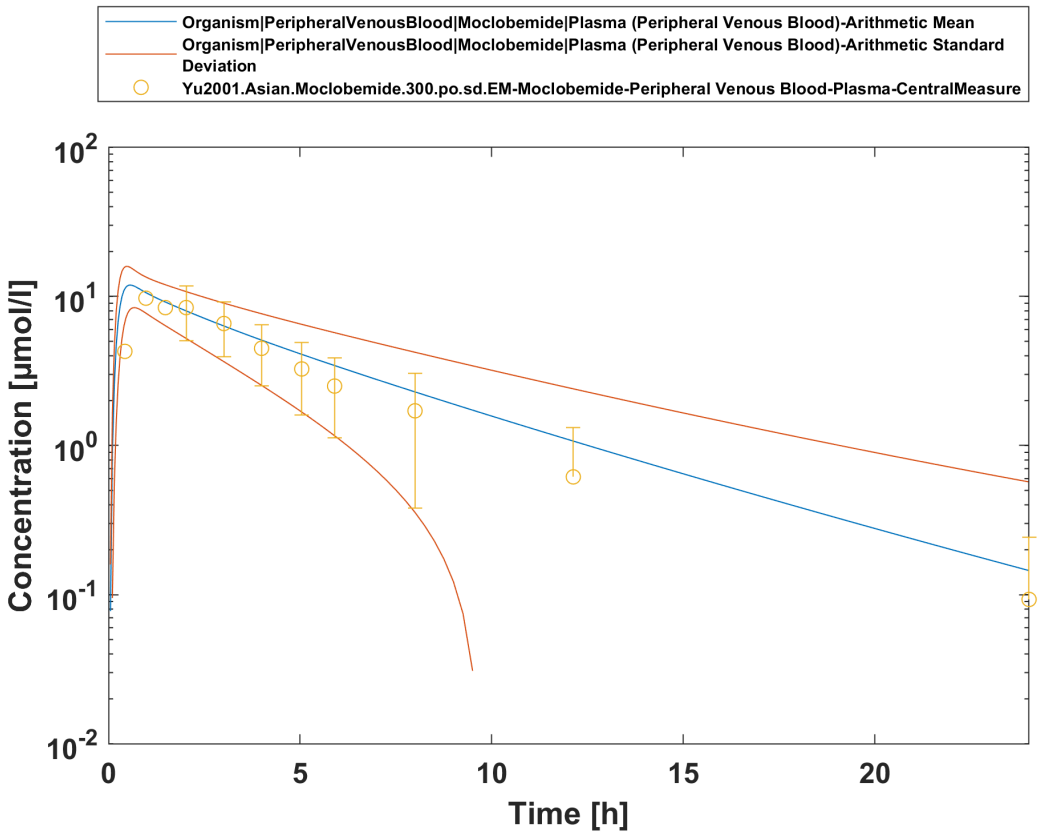

Time Profile Analysis

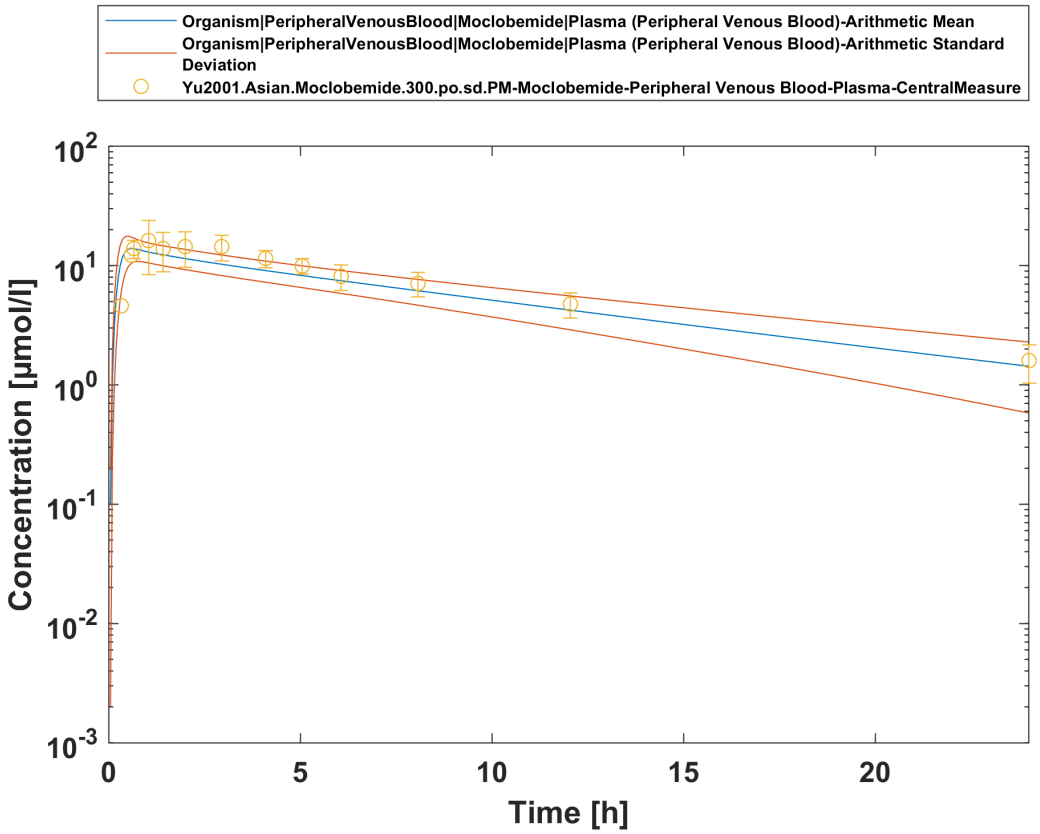

Time Profile Analysis

4 Conclusion

The developed PBPK model of moclobemide describes the observed concentration-time courses very well.

As most of the non-CYP2C19 metabolism is via FMO3 which is mainly expressed in the liver, non-CYP2C19 CL is modeled in the liver only.

Given not enough data to evaluate inhibition of emerging moclobemide metabolites, auto-inhibition of moclobemide appears appropriate approximation.

5 References

Dingemanse 1998 Dingemanse J, Wallnöfer A, Gieschke R, Guentert T, Amrein R. Pharmacokinetic and pharmacodynamic interactions between fluoxetine and moclobemide in the investigation of development of the “serotonin syndrome”. Clin Pharmacol Ther. 1998;63(4):403-413.

DrugBank DB01171 (https://www.drugbank.ca/drugs/DB01171)

Gram 1995 Gram LF, Guentert TW, Grange S, Vistisen K, Brøsen K. Moclobemide, a substrate of CYP2C19 and an inhibitor of CYP2C19, CYP2D6, and CYP1A2: A panel study. *Clinical Pharmacology & Therapeutics*. 1995 Jun;57(6):670–7.

Guentert 1990 Guentert TW, Tucker G, Korn A, Pfefen JP, Haefelfinger P, Schoerlin MP. Pharmacokinetics of moclobemide after single and multiple oral dosing with 150 milligrams 3 times daily for 15 days. Acta Psychiatr Scand. 1990;82(S360):91-93.

Hoskins 2001 Hoskins J, Shenfield G, Murray M, Gross A. Characterization of moclobemide N - oxidation in human liver microsomes. Xenobiotica. 2001 Jan;31(7):387–97.

IPCS ICHEM Website: https://inchem.org/documents/pims/pharm/pim151.htm#SectionTitle:3.3%20%20Physical%20properties

Ignjatovic 2009 Ignjatovic AR, Miljkovic B, Todorovic D, Timotijevic I, Pokrajac M. Moclobemide monotherapy vs. combined therapy with valproic acid or carbamazepine in depressive patients: A pharmacokinetic interaction study. Br J Clin Pharmacol. 2009;67(2):199-208.

Kuepfer 2016 Kuepfer L, Niederalt C, Wendl T, Schlender JF, Willmann S, Lippert J, Block M, Eissing T, Teutonico D. Applied Concepts in PBPK Modeling: How to Build a PBPK/PD Model.CPT Pharmacometrics Syst Pharmacol. 2016 Oct;5(10):516-531.

Kramer-Nielsen 1996 Kramer-Nielsen KK, Flinois JP, Beaune P, Brøsen K. The biotransformation of clomipramine in vitro, identification of the cytochrome P450s responsible for the separate metabolic pathways. *J Pharmacol Exp Ther*. 1996 Jun;277(3):1659–64.

Mayersohn 1995 Mayersohn M, Guentert TW. Clinical Pharmacokinetics of the Monoamine Oxidase-A Inhibitor Moclobemide*, Clinical Pharmacokinetics*. 1995 Nov;29(5):292–332.

MHRA Label Moclobemide MHRA label of Moclobemide film-coated tablets. Website: http://www.mhra.gov.uk/home/groups/par/documents/websiteresources/con097060.pdf

Moclobemide, INCHEM, Website https://inchem.org/documents/pims/pharm/pim151.htm#PartTitle:3.%20%20PHYSICO-CHEMICAL%20PROPERTIES

Nair 1993 Nair NPV, Ahmed SK, Ng Ying Kin NMK. Biochemistry and pharmacology of reversible inhibitors of MAO-A agents: Focus on moclobemide. *J Psychiatry Neurosci*. 1993;18(5):214-225.

PK-Sim Ontogeny Database Version 7.3 (https://github.com/Open-Systems-Pharmacology/OSPSuite.Documentation/blob/38cf71b384cfc25cfa0ce4d2f3addfd32757e13b/PK-Sim%20Ontogeny%20Database%20Version%207.3.pdf)

Pons 1990 Pons G, Schoerlin MP, Tam Y. Moclobemide excretion in human breast milk. *Br J Clin Pharmacol*. 1990;29(1):27–31.

Raaflaub 1984 Raaflaub J, Haefelfinger P, Trautmann KH. Single-dose Pharmacokinetics of the MAO-Inhibitor Moclobemide in Man. *Drug Res*. 1984; 34:80–2.

Schoerlin 1987 Schoerlin M-P, Mayersohn M, Korn A, Eggers H. Disposition kinetics of moclobemide, a monoamine oxidase-A enzyme inhibitor: Single and multiple dosing in normal subjects. *Clinical Pharmacology and Therapeutics*. 1987 Oct;42(4):395–404.

Wiesel 1985 Wiesel FA, Raaflaub J, Kettler R. Pharmacokinetics of oral moclobemide in healthy human subjects and effects on MAO-activity in platelets and excretion of urine monoamine metabolites. Eur J Clin Pharmacol. 1985;28(1 Supplement):89-95.

Willmann 2007 Willmann S, Höhn K, Edginton A, Sevestre M, Solodenko J, Weiss W, Lippert J, Schmitt W. Development of a physiology-based whole-body population model for assessing the influence of individual variability on the pharmacokinetics of drugs. *J Pharmacokinet Pharmacodyn* 2007, 34(3): 401-431.

Wu 2014 Wu F, Gaohua L, Zhao P, Jamei M, Huang S-M, Bashaw ED, et al. Predicting Nonlinear Pharmacokinetics of Omeprazole Enantiomers and Racemic Drug Using Physiologically Based Pharmacokinetic Modeling and Simulation: Application to Predict Drug/Genetic Interactions. *Pharmaceutical Research*. 2014 Aug;31(8):1919–29.

Yu 2001 Yu K, Yim DS, Cho J-Y, Park SS. Effect of omeprazole on the pharmacokinetics of moclobemide according to the genetic polymorphism of CYP2C19. Clinical Pharmacology & Therapeutics. 2001 Apr;69(4):266–73.

6 Glossary

ADME	Absorption, Distribution, Metabolism, Excretion
AUC	Area under the plasma concentration versus time curve
AUCinf	AUC until infinity
AUClast	AUC until last measurable sample
AUCR	Area under the plasma concentration versus time curve Ratio
b.i.d.	Twice daily (bis in diem)
CL	Clearance
Clint	Intrinsic liver clearance
Cmax	Maximum concentration
CmaxR	Maximum concentration Ratio
CYP	Cytochrome P450 oxidase
CYP1A2	Cytochrome P450 1A2 oxidase
CYP2C19	Cytochrome P450 2C19 oxidase
CYP3A4	Cytochrome P450 3A4 oxidase
DDI	Drug-drug interaction
e.c.	Enteric coated
EE	Ethinylestradiol
EM	Extensive metabolizers
fm	Fraction metabolized
FMO	Flavin-containing monooxygenase
fu	Fraction unbound
FDA	Food and Drug administration
GFR	Glomerular filtration rate
HLM	Human liver microsomes
hm	homozygous
ht	heterozygous
IM	Intermediate metabolizers
i.v.	Intravenous
IVIVE	In Vitro to In Vivo Extrapolation
Ka	Absorption rate constant
kcat	Catalyst rate constant
Ki	Inhibitor constant
Kinact	Rate of enzyme inactivation
Km	Michaelis Menten constant
m.d.	Multiple dose
OSP	Open Systems Pharmacology

ADME	Absorption, Distribution, Metabolism, Excretion
PBPK	Physiologically-based pharmacokinetics
PK	Pharmacokinetics
PI	Parameter identification
PM	Poor metabolizers
RT-PCR	Reverse transcription polymerase chain reaction
p.o.	Per os
q.d.	Once daily (quaque diem)
SD	Single Dose
SE	Standard error
s.d.SPC	Single dose Summary of Product Characteristics
SD	Standard deviation
TDI	Time dependent inhibition
t.i.d	Three times a day (ter in die)
UGT	Uridine 5'-diphospho-glucuronosyltransferase
UM	Ultra-rapid metabolizers